

## DIRECTIVITY PATTERN OPTIMIZATION OF DIGITAL HEARING AID BY BOUNDARY ELEMENT METHOD

Soon Suck Jarng

ssjarng@chosun.ac.kr

Chosun University

Dept. of Information, Control & Instrumentation,  
Chosun University, 375 Seoseok-Dong Dong-Ku  
Gwnag-Ju, 501-759, South Korea

You Jung Kwon

avaskorea@yahoo.co.kr

Chosun University

Dept. of Information, Control & Instrumentation,  
Chosun University, 375 Seoseok-Dong Dong-Ku  
Gwnag-Ju, 501-759, South Korea

### ABSTRACT

The noise reduction of the ITE (In-The-Ear) hearing aid (HA) can be achieved by an array of microphones. Each of the right and the left ears is fixed with two ITE HA microphones. This two HA microphones' array produces particular patterns of directivity which geometrically increases the S/N ratio. The boundary element method (BEM) was used for the three dimensional modeling and optimization of the human head model directivity pattern with the two by two microphone arrays. Three particular structures of the head model were considered; sphere, head I, head II. All three structures were meshed for boundary surface element grids. Head model I element meshing was generated from three dimensional laser scanned points' data. And Head model II element meshing was formed by a CAD program. This numerical analysis was then applied for the calculation of the time delay parameters of the digital hearing aid DSP chip. The separation between two microphones was fixed to 10 mm. Input frequencies are 500, 1000, 1500, 2000, 2500, 3000, 3500, 4000 Hz. Time delays between two microphones were changed to produce the most narrow directivity pattern in the fore front of the head. The variation of the time delay was examined in accordance with input frequencies.

**Keywords:** Human head model, Boundary element method, Directivity pattern simulation, Hearing Aids

### 1 INTRODUCTION

One of the advanced features of the digital hearing aid (HA) chip is its parameter adjusting function. The user can change the parameter values of the digital HA chip in order to raise the performance of some particular HA functioning. Of course the main function of the HA is the amplification of the electrical signal. There are also many other specifications, but one particular feature we consider in this paper is the time delaying between two input channels. The outputs of two microphones can be input into a HA DSP chip such as Gennum GB3211 [1]. Two microphones are used for making directional HAs [2]. The directional HA may have the increased sensitivity to the sound coming from a particular direction. This geometrical feature effectively improves the noise reduction in the presence of

environmental noise. Each of the right and the left ears may have an ITE HA with two microphones. These two twin microphones' array simultaneously activates the formation of the directivity pattern. The directivity pattern of the digital HA can be changed depending on how those four microphones are located. It is common that each pair of two microphones has a short space of separation and that both the right and the left ears would have the same type of digital HAs. But there is a comparatively long space of the head between two ears.

Then a question arises. That is how much we have to have the short space between two microphones once we know the size of the head in order to produce the most directive sensitivity pattern. Or how much is the time delay between two microphones if we fix the space distance? We applied the boundary element method (BEM) for the solution of the question. The numerical method will be very briefly mentioned and be followed by the application of the present problem.

### 2 BOUNDARY ELEMENT METHOD (BEM)

The sound pressure is scattered when an incident sound pressure is hit on an object such as the head. Then the sound field around the head is mixed with both the incident sound pressure and the scattered sound pressure. The target of the numerical method is to calculate the mixed sound pressure around the head. The size and the shape of the head and the ear as well as the input frequency may affect the geometrical variation of the sound pressure field.

The boundary element solution of the sound pressure field is based on the Helmholtz partial differential equation [3]. For sinusoidal steady-state problems, the Helmholtz equation,  $\nabla^2\Psi + k^2\Psi = 0$  represents the fluid mechanics.  $\Psi$  is the acoustic pressure with time variation,  $e^{j\omega t}$ . In order to solve the Helmholtz equation in an infinite air media, a solution to the equation must not only satisfy structural surface boundary condition (BC),  $\partial\Psi/\partial n = \rho_f \omega^2 a_n$  but also the radiation condition at infinity,  $\lim_{|r|\rightarrow\infty} \int_S (\partial\Psi/\partial r + jk\Psi)^2 dS = 0$ .  $\partial/\partial n$  represents

differentiation along the outward normal to the boundary.  $a_n$  is normal displacement.

The Helmholtz integral equation derived from Green's second theorem provides such a solution for radiating pressure waves;

$$\oint_S \left( \Psi(q) \frac{\partial G_k(p,q)}{\partial n_q} - G_k(p,q) \frac{\partial \Psi(q)}{\partial n_q} \right) dS_q = \beta(p) \Psi(p) \quad (1)$$

where  $G_k(p,q) = e^{-jkr} / 4\pi r$ ,  $r = |p - q|$

$p$  is any point in either the interior or the exterior and  $q$  is the surface point of integration.  $\beta(p)$  is the exterior solid angle at  $p$ .  $k$  is wave number.

The discrete BEM formulation of the Helmholtz surface integral equation can be represented as

$$\{\Psi\} = +\rho_f \omega^2 [A]^{-1} [B] \{a\} - [A]^{-1} \{\Psi_{inc}\} \quad (2)$$

where  $\rho_f$  is the air density and  $\Psi_{inc}$  is the incident sound pressure.  $[A]$  and  $[B]$  are acoustic impedance matrices [4].

Each three dimensional boundary surface element is composed of 8 quadratic nodes and each node has nodal surface pressure ( $\Psi$ ) variable. If we assume a rigid surface boundary condition, equation (2) becomes

$$\{\Psi\} = -[A]^{-1} \{\Psi_{inc}\} \quad (3)$$

Once  $\{\Psi\}$  is known, the acoustic pressure in the near or far field is determined by  $\beta(p)=1$  of equation (1) for given values of surface nodal pressure and zero surface nodal displacement;

$$\Psi(p_i) = \sum_{m=1}^{nt} \sum_{j=1}^8 A^i_{m,j} \Psi_{m,j} \quad (4)$$

where  $nt$  is the total number of the boundary elements.

### 3 BOUNDARY ELEMENT MESH GENERATION

Three particular head-like structures were considered; sphere, head I CAD model, head II arbitrary shape model. All three structures were meshed for boundary surface element grids. Head I model element mesh was formed by a CAD program. Head II model element mesh was generated from three dimensional laser scanned points' data [5].

Figure 1 shows the surface element meshes of a sphere. The diameter of the sphere is 18cm. Figure 1(b) shows the magnified view of two microphones indicated by an arrow of Fig. 1(a). Figure 1(c) shows each twin microphones in the left ear and the right ear. For initial convenience the spherical head model oversimplifies the head and the ear structures. The y axis indicator of Fig. 1(c) directs toward the fore front of the head and the other

side is assumed to be the backward of the head. The angle of the directivity pattern starts from the front in anti-clockwise direction.

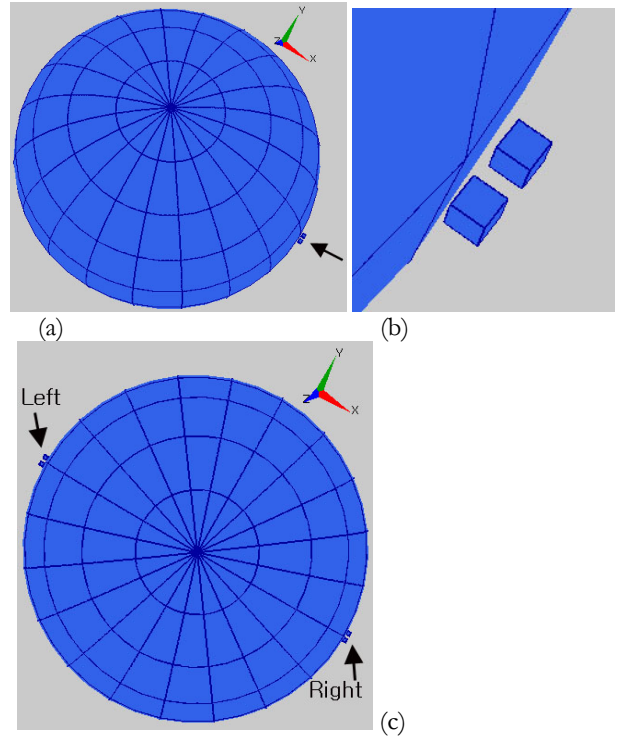


Fig. 1 (a) The surface element mesh of a sphere (Diameter = 18cm). (b) The magnified view of two microphones indicated by an arrow of (a). (c) Each twin microphones in the left ear and the right ear.

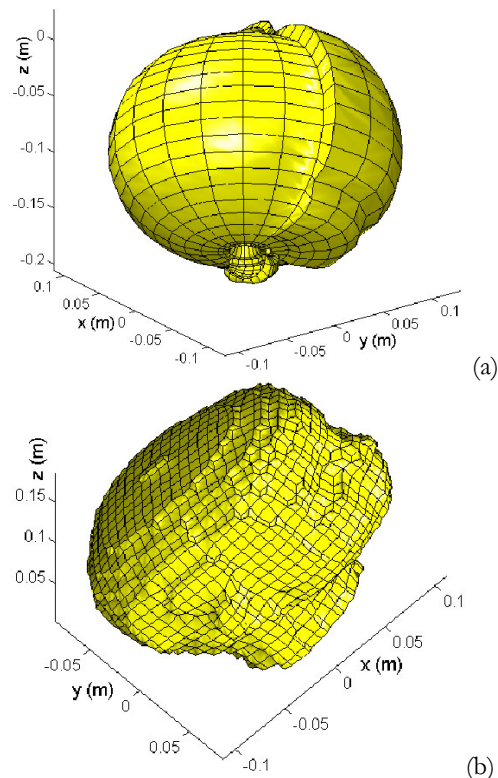


Fig. 2 Head models I and II. (a) Head model I generated by a CAD program (Diameter = 18cm). (b) Head model II generated by an automatic mesh generation program (Diameter = 18cm).

Figure 2 shows head models I and II. Both models are meshed for surface boundary elements. Figure 2(a) shows a head model I generated by a CAD program. The head model I has the outer ear and the ear carnal, and the diameter of the head model I from the front to the back is 18cm. Figure 2(b) shows a head model II generated by an automatic mesh generation program developed by the author. The automatic mesh generation program is based on many point data in three dimensional coordinates measured by a three dimensional laser scanner.

The BEM program was coded in Fortran in double precision and was executed by a PC with 2G RAM. The air density is 1.34 [Kg/m<sup>3</sup>] and the sound speed in the air is 344 [m/sec]. Input frequencies are 500, 1000, 1500, 2000, 2500, 3000, 3500, 4000 Hz.

### 4 RESULTS

Figure 3 shows the near filed of the sound pressure for the sphere model at 1 kHz. The upper side is the front and the lower side is the rear in two dimensions. The incident sound pressure is coming from the front.

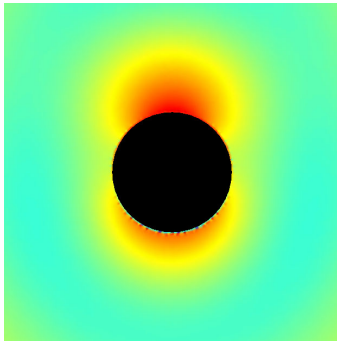


Fig. 3 The near filed of the sound pressure for the sphere model at 1 kHz in two dimensional view.

Figure 4 shows directivity patterns of two front and rear microphones only without the spherical head model. The distance between two microphones is 10mm. The input frequency,  $f$ , is 4kHz. The rear microphone is set to be a reference microphone, so as to have zero time delay. The time delays,  $\Delta t$ , between the front and the rear microphones are (a) 0, (b) 0.0875, (c) 0.1, (d) 0.1125, (e) 0.1375, (f) 0.15, (g) 0.1625, (i) 0.175 in milliseconds. The amplitude and the phase of the front microphone is  $A_f$  and  $\theta_f$  while those of the rear microphone is  $A_r$  and  $\theta_r$ . The strength of the summed sound pressure from the front and the rear microphones is calculated as;

$$\left| A_r \cos(2\pi f \cdot (t - 0) + \theta_r) + A_f \cos(2\pi f \cdot (t - \Delta t) + \theta_f) \right| \quad (5)$$

The front microphone is delayed in time because it leads the phase. Figure 4 shows that the directivity pattern of the two microphones' array looks like symmetric omnidirectional shape in zero time delay. As the time delay increases, the directivity pattern changes in its shape but returns back to its initial shape due to periodicity. The present digital HA considers the directivity pattern effect of the two microphones only for each ear. It do not consider the effects of the head and the ear as well as the size and the shape.

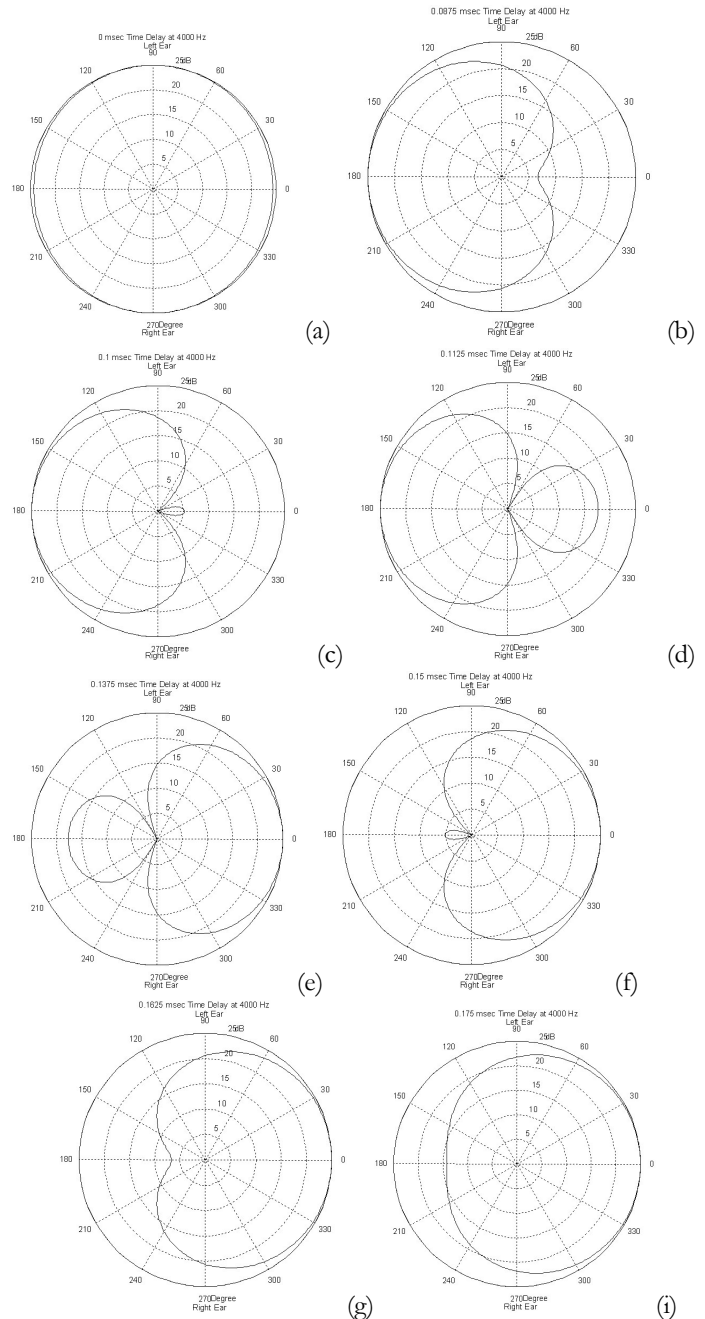
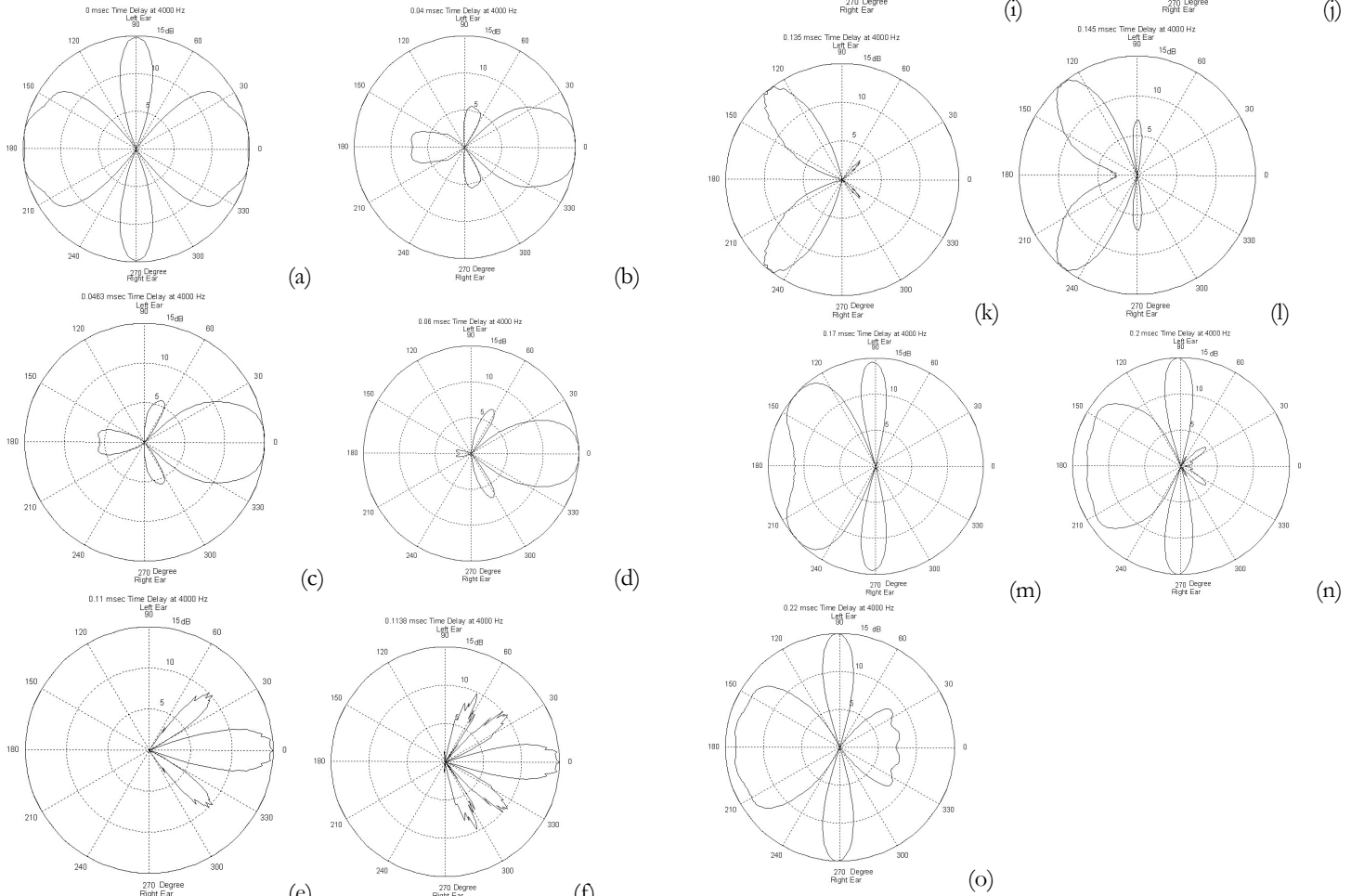


Fig. 4 Directivity patterns without spherical head model. Microphone separation=10mm. Input frequency=4kHz. Time delays [msec]= (a) 0, (b) 0.0875, (c) 0.1, (d) 0.1125, (e) 0.1375, (f) 0.15, (g) 0.1625, (i) 0.175. Reference microphone (0 time delay) = Rear Microphone.

Figure 5 shows directivity patterns of two twin microphones with the spherical head model effect. The distance between two microphones is 10mm. The input frequency,  $f$ , is 4kHz. The time delays between the front and the rear microphones are (a) 0, (b) 0.04, (c) 0.0463, (d) 0.06, (e) 0.11, (f) 0.1138, (g) 0.115, (h) 0.1163, (i) 0.12, (j) 0.125, (k) 0.135, (l) 0.145, (m) 0.17, (n) 0.2, (o) 0.22. Because of the geometrical effect the sphere head, the directivity patterns of the two twin microphones with the sphere head show different shapes in comparison with the two microphones without the sphere head. The strength of the summed sound pressure from the two twin microphones is calculated as;

$$|A_r^r \cos(2\pi f \cdot (t-0) + \theta_r^r) + A_r^l \cos(2\pi f \cdot (t-\Delta t) + \theta_r^l)| \times |A_l^r \cos(2\pi f \cdot (t-0) + \theta_l^r) + A_l^l \cos(2\pi f \cdot (t-\Delta t) + \theta_l^l)| \quad (6)$$

where  $A_r^r$  and  $\theta_r^r$  are the amplitude and the phase of the right ear microphones while  $A_l^l$  and  $\theta_l^l$  are those of the left ear microphones.



*Fig. 5 Directivity patterns with spherical head model. Microphone separation=10mm. Input frequency=4kHz. Time delays [msec]= (a) 0, (b) 0.04, (c) 0.0463, (d) 0.06, (e) 0.11, (f) 0.1138, (g) 0.115, (h) 0.1163, (i) 0.12, (j) 0.125, (k) 0.135, (l) 0.145, (m) 0.17, (n) 0.2, (o) 0.22. Reference microphone (0 time delay) = Rear Microphone.*

Figure 7 indicates that the time delay of the digital HA needs to be varied as a function of the frequency if the user wants to have sharp directivity patterns in wide bandwidth. This suggests that a precisely controlled phase delay circuit should be included inside the digital HA for better directivity performance.

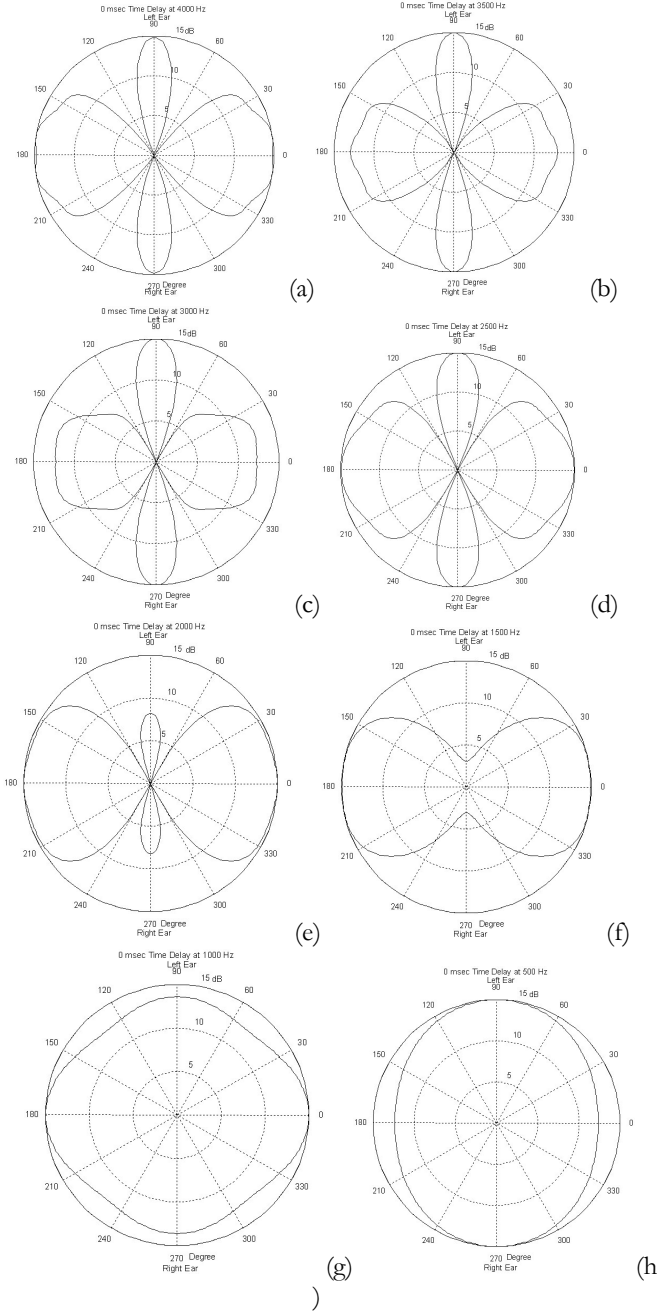


*Fig. 6 Directivity patterns of the spherical head model. Microphone separation=10mm. Time delays [msec]=0. Input frequencies= (a) 4000 Hz, (b) 3500 Hz, (c) 3000 Hz, (d) 2500 Hz, (e) 2000 Hz, (f) 1500 Hz, (g) 1000 Hz, (h) 500 Hz.*

Figure 6 shows directivity patterns of the spherical head model. The time delay between the front and the rear microphones is fixed to be zero but the input frequency is changed from 4kHz down to 0.5kHz. As the input frequency decreases the directivity pattern becomes omnidirectional because of increased wave length.

Figure 7 shows directivity patterns of the spherical head model. Particular time delay is applied to produce the most sharp directivity pattern in accordance with each input frequency.

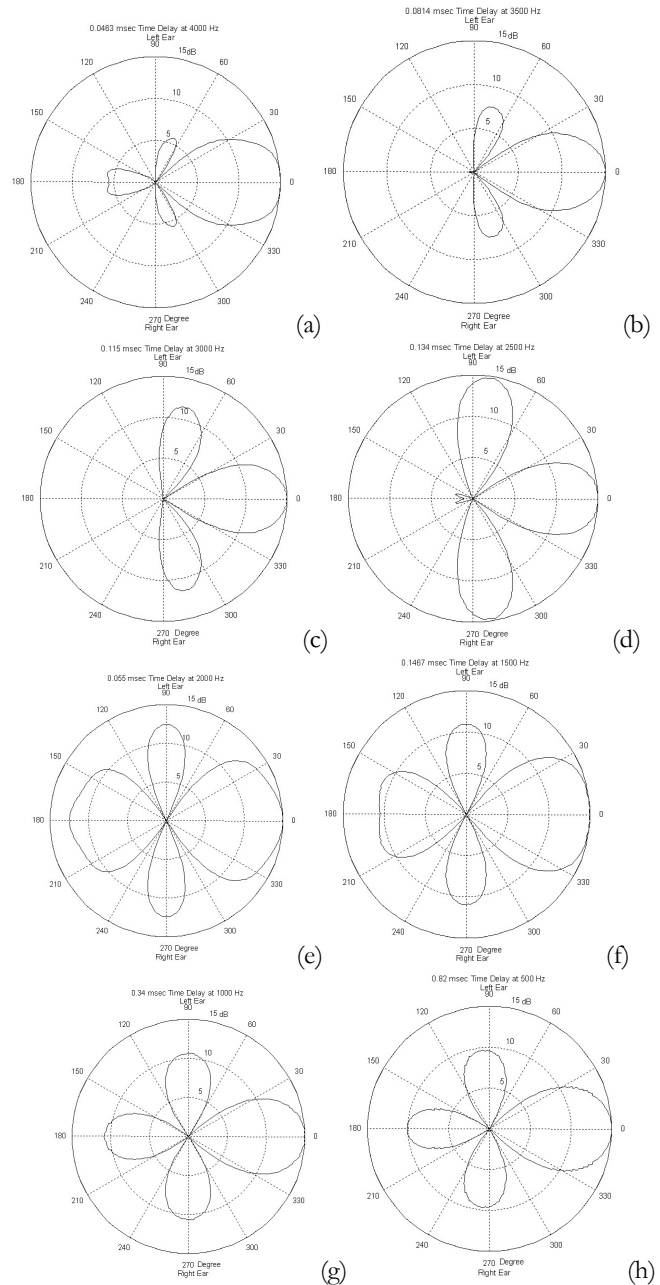


*Fig. 7 Directivity patterns of the spherical head model. Microphone separation=10mm. Time delays [msec] & Frequencies [Hz]= (a) 0.0463 & 4000, (b) 0.0814 & 3500, (c) 0.115 & 3000, (d) 0.134 & 2500, (e) 0.055 & 2000, (f) 0.1467 & 1500, (g) 0.34 & 1000, (h) 0.82 & 500.*

Figure 8 shows the surface sound pressure distribution of the sphere model at the oncoming incident sound pressure.

Figure 8(a) has  $0^\circ$  incident sound pressure while Figure 8(b) has  $90^\circ$  incident sound pressure directions.

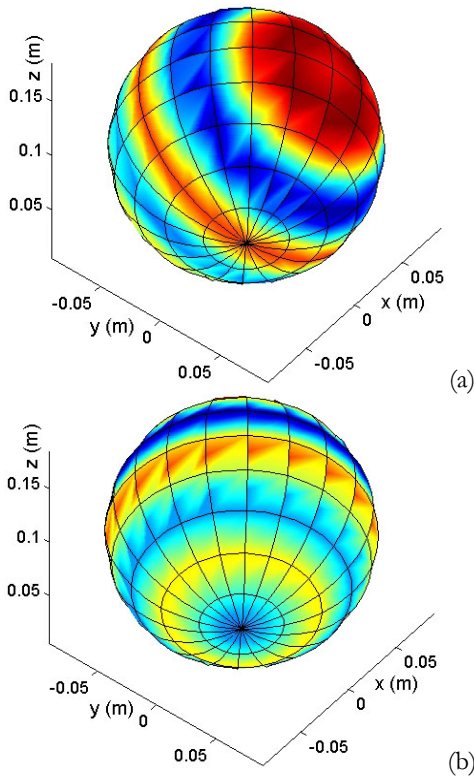


Fig. 8 The surface sound pressure distribution of the sphere model at the oncoming incident sound pressure. (a)  $0^\circ$ , (b)  $90^\circ$  incidence.

Figure 9 shows directivity patterns of the sphere model in polar and in rectangular form. Figure 9 (a) and (b) are for zero time delay, and (c) and (d) are for 0.04625 [msec] time delay. The input frequency is 4 kHz. The time delay of 0.04625 [msec] is equivalent to 18.5% in 4kHz periodic phase.

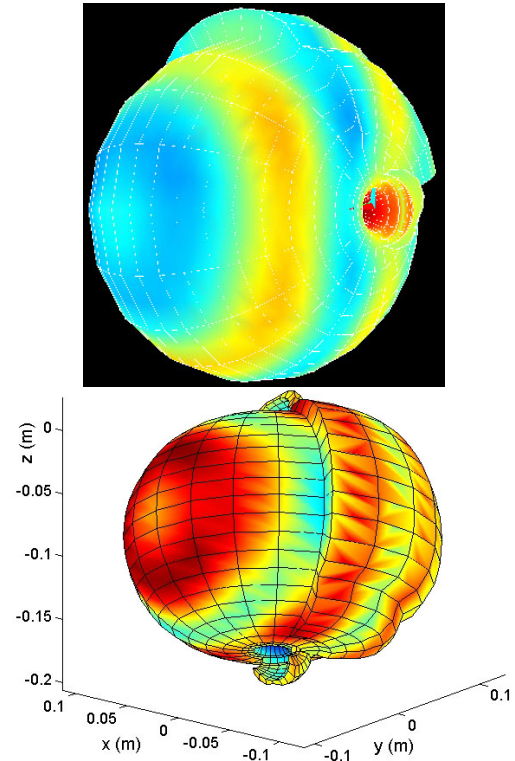


Fig. 10 The surface sound pressure distribution of the head and ear model I at the  $0^\circ$  oncoming incident sound pressure.

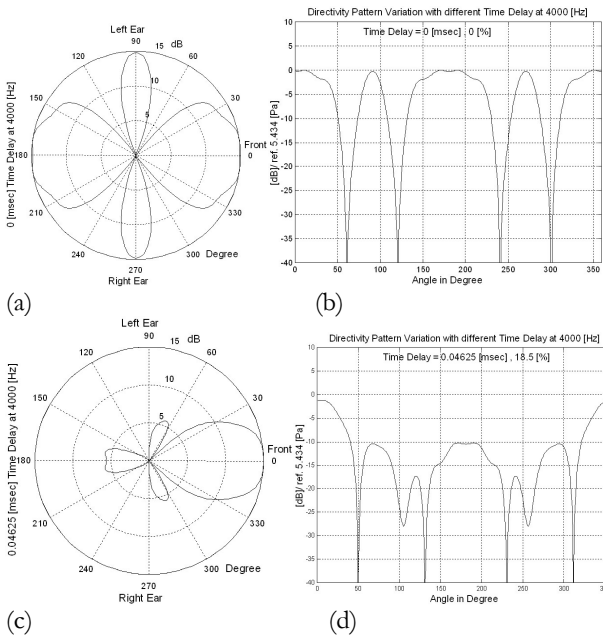


Fig. 9 Directivity patterns of the sphere model in polar and in rectangular form. (a) and (b) for zero time delay. (c) and (d) for 0.04625 [msec] time delay. Input frequency = 4 kHz.

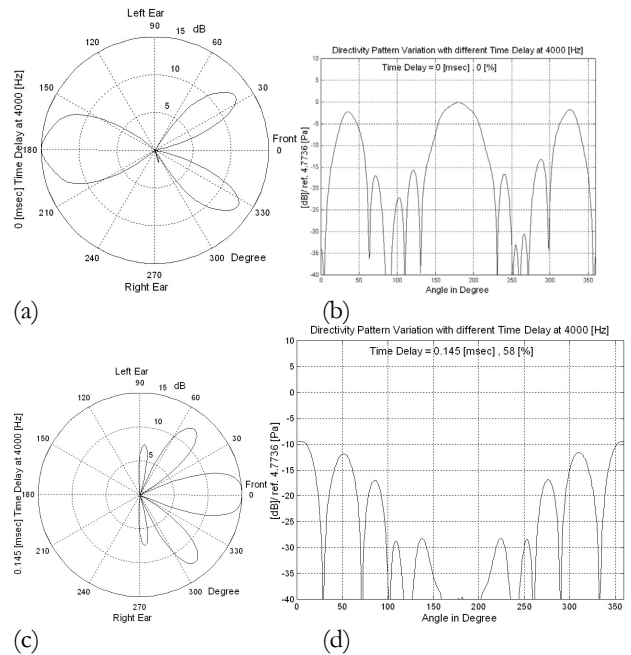


Fig. 11 Directivity patterns of the head and ear model I in polar and in rectangular form. (a) and (b) for zero time delay. (c) and (d) for 0.145 [msec] time delay. Input frequency = 4 kHz;

Figure 10 shows the surface sound pressure distribution of the head and ear model I at the  $0^{\circ}$  oncoming incident sound pressure. And Figure 11 shows directivity patterns of the head and ear model I in polar and in rectangular form. Figure 11 (a) and (b) are for zero time delay, and (c) and (d) are for 0.145 [msec] time delay. The input frequency is 4 kHz. The time delay of 0.145 [msec] is equivalent to 58% in 4kHz periodic phase. The particular time delay is chosen to produce the most sharp directivity pattern. This difference of the time delay between Fig. 9 (c) and Fig. 11 (c) may indicate that the shape and the size of the head and the ear affect the degree of the time delay.

Figure 12 shows the head model II generated from three dimensional co-ordinates point data. In this head model II, the outer ears are not clearly meshed for resonance effects, that is, both outer ears are closed.

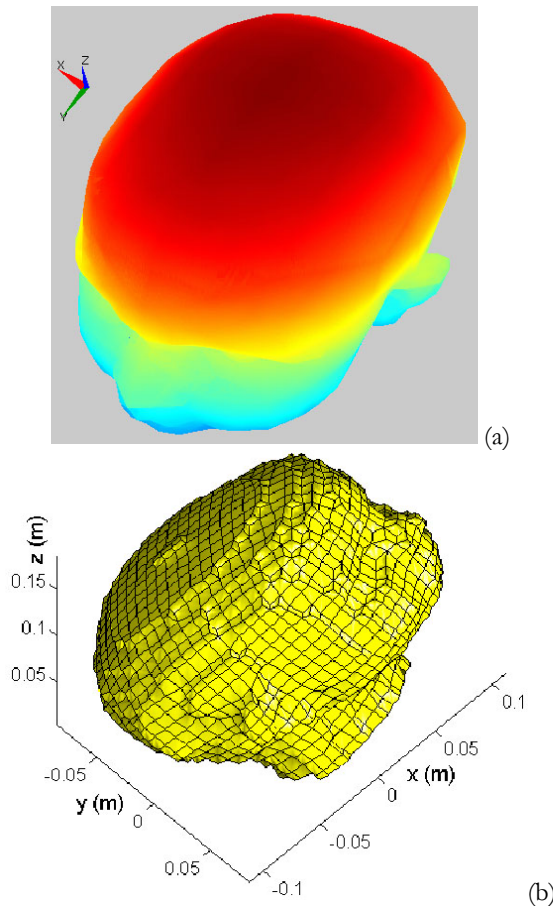


Fig. 12 The head model II. (a) Three dimensionally measured scanned point data. (b) Mesbed surface boundary elements.

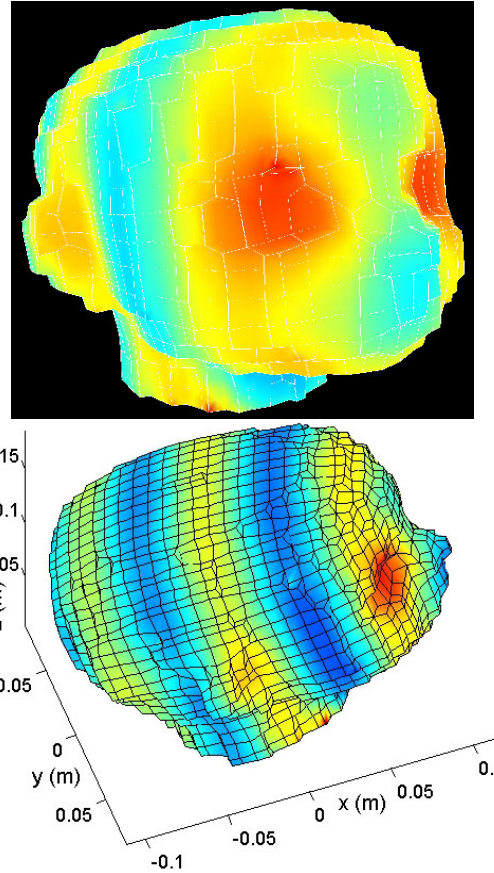


Fig. 13 The surface sound pressure distribution of the head model II at the  $0^{\circ}$  oncoming incident sound pressure.

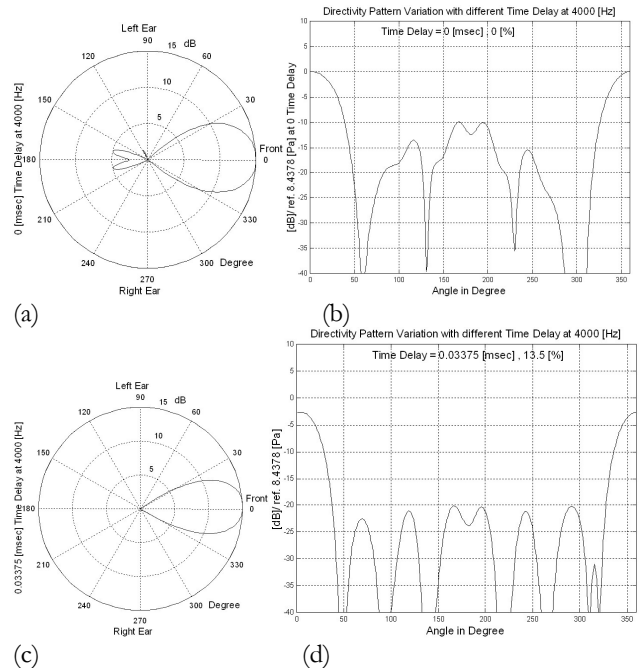


Fig. 14 Directivity patterns of the head model II in polar and in rectangular form. (a) and (b) for zero time delay. (c) and (d) for 0.03375 [msec] time delay. Input frequency = 4 kHz.

Figure 13 shows the surface sound pressure distribution of the head model II at the  $0^\circ$  oncoming incident sound pressure. And Figure 14 shows directivity patterns of the head model II in polar and in rectangular form. Figure 21 (a) and (b) are for zero time delay, and (c) and (d) are for 0.03375 [msec] time delay. The input frequency is 4 kHz. The time delay of 0.03375 [msec] is equivalent to 13.5% in 4kHz periodic phase. The particular time delay is chosen to produce the most sharp directivity pattern as previous figures showed.

## 5 CONCLUSION

In Figure 7 it was indicated that the time delay of the digital HA needs to be varied as a function of the frequency. The author suggests that a precisely controlled phase delay circuit should be included inside the digital HA for better directivity performance. The shape and the size of the head and the ear may affect the directivity performance of the digital HA. This means that the amplitude envelope of the HA amplification needs to include those geometrical effects of the head and the ear. It is physically difficult to vary the position of the twin microphones, but the time delay of the digital HA may be changed not only as a function of frequency but also as a function of the geometric parameter of the head and the ear shape and size. Then the BEM could be further applied as a parameter extraction tool for the precise control of the time delay in the digital HA. The BEM can be applied for the sound pressure field calculation for any arbitrary shape of the head and the ear.

## 6 ACKNOWLEDGMENTS

This study was supported by research fund from MOST Korea (Industrial Analysis Software Development Project, 3<sup>rd</sup> Year), 2003.

## 7 REFERENCES

- [1] Jarng S.S., “*Gennum GB3211 ITE Hearing Aid Chip Interface and Electro-Acoustic Testing*”, Proc. of Korean Sensor Society, Vol. 14, pp. 59-62, 2003.
- [2] Frye G. J., “*Testing Digital and Analog Hearing Instruments: Processing Time Delays and Phase Measurement*”, The Hearing Review, Vol. 8, pp. 1-8, 2001.
- [3] Francis D.T.I., “*A boundary element method for the analysis of the acoustic field in three dimensional fluid-structure interaction problems*”, Proc. Inst. of Acoust., Vol. 12, Part 4, pp.76-84, 1990.
- [4] Francis D.T.I., “*A gradient formulation of the Helmholtz integral equation for acoustic radiation and scattering*”, J. Acoust. Soc. Am. Vol. 93(4), Part 1, pp. 1700-1709, 1993.
- [5] Lee Seok-Hee, Kim Ho-Chan, Hur Sung-Min, Yang Dong-Yol, “*STL file generation form measured point data by segmentation and Delaunay triangulation, Computer-Aided Design*”, Vol.34, No.10, pp. 691-704, 2002.